Available online at www.sciencedirect.com
SCIENCE DIRECT®
Earth and Planetary Science Letters 242 (2006) 365–374
EPSL
www.elsevier.com/locate/epsl

Constraints on 2004 Sumatra–Andaman earthquake rupture from GPS measurements in Andaman–Nicobar Islands

V.K. Gahalaut [a,*], B. Nagarajan [b], J.K. Catherine [a], S. Kumar [b]

[a] *National Geophysical Research Institute, Uppal Road, Hyderabad 500007, India*
[b] *Geodetic and Research Branch, Survey of India, Dehradun 248 001, India*

Received 27 September 2005; received in revised form 25 November 2005; accepted 27 November 2005
Available online 19 January 2006
Editor: R.D. van der Hilst

Abstract

The 26 December 2004 Sumatra–Andaman earthquake (Mw 9.0–9.3) is the greatest earthquake of the modern seismological era. The rupture characteristics of the earthquake, particularly in the Andaman–Nicobar region, are not well resolved from seismological or far-field geodetic data. Here, in this article we present, campaign mode Global Positioning System (GPS) measurements of coseismic displacements at 13 sites in the Andaman–Nicobar Islands before and after the 2004 Sumatra–Andaman earthquake. These measurements provide improved estimates of rupture characteristics in the region. Coseismic horizontal ground displacement of 1.5–6.5 m towards the southwest and coseismic vertical displacement, mostly subsidence, of 0.5–2.8 m occurred along the Andaman–Nicobar Islands with maximum displacements in the Nicobar Islands. We estimate coseismic slip under the Andaman and Nicobar Islands as 3.8–7.9 m and 11–15 m, respectively. The length of the rupture is estimated to be about 1500 km with a width varying from 120 km under Middle Andaman Island to 160 km under Great Nicobar Island. GPS measurements during January 11–22, 2005 from Port Blair suggest rapid afterslip in the postseismic period. Limited GPS data available from 1995 measurements at two sites in Andaman provide evidence of strain accumulation that varied significantly in the 10 yr preceding the earthquake.

Keywords: Sumatra–Andaman earthquake; GPS measurements; coseismic displacements; Andaman–Nicobar Islands; rupture characteristics

1. Introduction

The 26 December 2004 giant Sumatra–Andaman earthquake (Mw 9.0–9.3) occurred in the Sumatra–Andaman subduction zone where the Indo-Australian plate underthrusts the Burmese plate [1,2]. The motion of Indian plate relative to Sunda plate is about 4 cm/yr towards N20°E while that of Australian plate in the northern Sumatra region is about 5 cm/yr towards N8°E [3]. The oblique motion between the Indo-Australia and Burma–Sunda plates is accommodated through predominantly thrust motion in the Sumatra–Andaman trench region, and through predominantly strike-slip motion in the Andaman Sea ridge-transform system in the back arc region and the Sumatra fault system in the south [4,5,6]. The rate of convergence in the Andaman and Sumatra region is not well constrained and the estimate ranges from 14 to 68 mm/yr [6–10]. No great earthquake (M ≥ 8) has been reported from the Andaman–Nicobar and northern Sumatra region, though major events in 1847 (M 7.5), 1868, 1881 (M 7.9) and 1941 (M 7.7) have occurred in the region. Great earthquakes in 1797,

* Corresponding author. Tel.: +91 40 23434700; fax: +91 40 23434651.
E-mail address: vkgahalaut@yahoo.com (V.K. Gahalaut).

0012-821X/$ - see front matter © 2005 Elsevier B.V. All rights reserved.
doi:10.1016/j.epsl.2005.11.051

1861, 1833 and 2005 have been reported from the subduction zone near and southeast of Sumatra [2,11].

The 2004 Sumatra earthquake nucleated off the western coast of northern Sumatra and propagated north–northwest. Fast slip occurred in the southern part with a magnitude of slip reaching 15 m, which extended to the north–northwest direction at a velocity of 2.5 km/s, rupturing the 1300-km-long plate boundary in about 8–10 min [12]. The seismological data do not constrain slip on the rupture under Andaman–Nicobar islands reasonably well, as most of the slip in this part occurred at a time scale beyond the seismic band [2,12]. In the subsequent 1-h period, additional slow slip occurred in the Andaman–Nicobar region [1,2,13,14]. However, Ishii et al. [15], who used Hi-Net seismic array data from Japan, did not find evidence to support slow slip on the northern part of the rupture. Vigny et al. [3] also argued against slow slip and suggested that the entire displacement at GPS sites in the northern Thailand occurred in less than 10 min after the earthquakes. Using far-field GPS sites about 400–3000 km from the rupture, they derived a slip model for this earthquake. In addition to the far-field GPS data [3,14,16], rupture models have been constrained by data from five near-field sites in Andaman–Nicobar Islands [17]. Here, we improve resolution on slip and rupture characteristics using coseismic displacements derived from GPS data from 13 sites in Andaman–Nicobar islands. We provide evidence of postseismic deformation in the region and evidence of strain accumulation in the preceding 10 yr of the earthquake. Further, we discuss the possibility of earthquake triggering near the northern edge of the rupture.

2. GPS measurements and coseismic displacements

In 1994–95, the Survey of India (SOI) established 30 GPS sites in the Andaman and Nicobar Islands covering virtually every major island. In March 2004, 13 sites were again occupied. After the 26 December 2004 earthquake, 12 sites could be reoccupied as the site at Car-Nicobar was damaged by the earthquake and the tsunami. These sites are on the eastern coast of the islands (Fig. 1). The western coast of Andaman Island is mostly a reserved area for local tribes. The sites consist of either a steel pin cemented into bed rock or a mark on a L-shaped steel angle embedded in a concrete pillar of dimension of about 1 m × 1 m, reaching to bedrock. In the 12-day-long campaign of January 2005, the Port Blair site was continuously occupied throughout the survey. Daily 24-h GPS data files from the 12 sites were processed using GAMIT/GLOBK [18,19]. We also included IGS stations at HYDE, IISC, COCO, BAKO, DGAR, SAMP, NTUS, PIMO, KIT3, POL2 and WETZ in the processing. The last three sites were constrained to their ITRF coordinates. Coordinates of all the sites were estimated in the ITRF2000 reference frame. The coseismic displacements derived at IGS sites are reported in our earlier article [16]. Difference in coordinates of sites in the 2004 and 2005 surveys in Andaman–Nicobar Islands is mainly due to coseismic displacements. Due to the gap of about 10 months in the two measurements, the estimated displacement may contain contribution of secular plate motion of ~5 cm/yr [8–10] with reference to Indo-Australian plate, which is insignificant here. However, there could be some contribution from postseismic deformation as the measurements were carried out after about 2 weeks of the earthquake. Evidence of postseismic deformation can be seen at Port Blair (see Postseismic deformation) and in our subsequent campaign mode measurements in Andaman–Nicobar region. These measurements suggest that even in the postseismic period, the sites continued to move towards WSW, i.e., in the direction of coseismic displacement. Thus, the gap of 2 weeks in the GPS measurements after the earthquake must have led in overestimating the coseismic displacements. At sites in Thailand, Indonesia and Malaysia, the postseismic deformation in first 15 days is estimated to be about 10% of the coseismic displacement [3]. However, in the absence of any such direct measurements in Andaman–Nicobar region, we restrain ourselves to quantify it and assume it to be entirely coseismic. Coseismic displacements at these sites are shown in Fig. 1 and Table 1. For the coseismic displacement at Car-Nicobar, we have adopted the estimate provided by Jade et al. [17] as our site was damaged. Even at this site there may be contribution from postseismic deformation, as the measurements were made 2 months after the earthquake.

Horizontal displacement of about 4–6.5 m and subsidence of 1–2.8 m occurred in the Nicobar Islands. In the Andamans, horizontal displacement of 1.5–5.0 m occurred with an intervening low displacement of 1.5–2 m in Middle Andaman Island. Coseismic subsidence of less than a meter occurred in the Andaman except on North Andaman Island, where uplift of 0.5–1.0 m was estimated. We find that these displacements are consistent with the sparser observations of coseismic displacement from 5 GPS sites [17,20] and with the inferred pattern of subsidence and uplift derived from reports of apparent sea level changes [11,21,22].

Large displacements at all sites attest that the rupture extended up to the North Andaman Island. The direction of horizontal displacement vectors towards SWS (Fig. 1) suggests that the slip on the rupture was predominantly

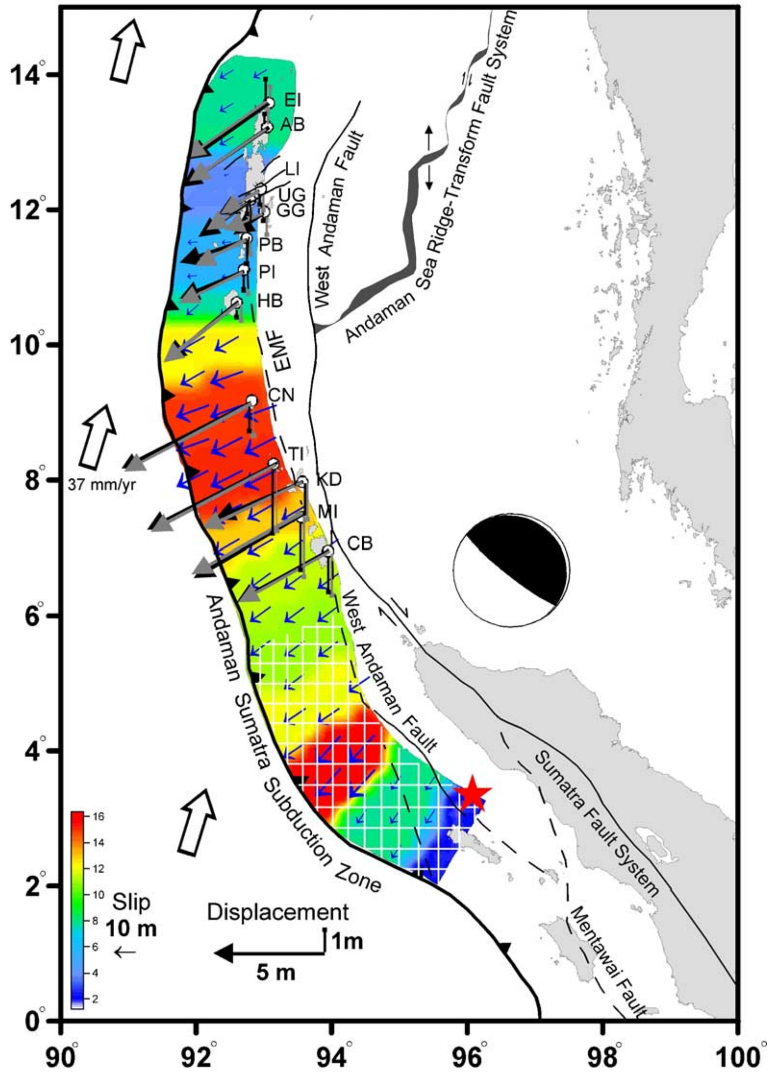

Fig. 1. GPS-derived coseismic displacements in the Andaman–Nicobar Islands and estimated slip on the 2004 Sumatra earthquake rupture. Red star marks the earthquake epicentre and the beachball shows the focal mechanism. Motion of Indian plate with respect to Sunda Plate as 37 mm/yr is also shown. Bold black arrows show the coseismic displacements at GPS sites (identified by two-letter abbreviations) from campaign mode measurements. The error ellipses are extremely small in comparison to the displacement magnitude, and hence are not shown. Vertical lines with blunt heads indicate subsidence or uplift at that site. Estimates of slip distribution on the subsurface rupture and the width of the rupture under the Andaman–Nicobar region are also shown. Slip on the hatched part of the rupture is not well resolved by these observations. Blue arrows on the rupture show slip direction (rake) along with the magnitude. Gray colour arrows are the simulated displacements at each site from the estimated slip distribution. Slip and width of the rupture in each segment can also be read from Table 2.

of thrust type in the Nicobar Islands, and became oblique in the Andaman Islands owing to the change in strike of the subduction zone. We suggest that the downdip edge of the rupture lie close to the east coast of the island belt [16]. This is consistent with (i) reports of uplift of the western coast of Andaman Island and North Sentinel Island [11,21,22], which lies 60 km west of Port Blair, and (ii) reports of coseismic subsidence on the east coast of the islands which decreased in the east, as seen at GG at Havelock Island, which is to the east of the LI and UG at Middle Andaman (Table 1) and at KD at Kardip, which is to the east of TI at Teresa Island.

3. Analysis of coseismic displacement for rupture characteristics

We used the horizontal and vertical coseismic displacements at 13 sites to estimate coseismic slip on a fault model assuming an elastic half-space [23]. Looking at the similarity in the magnitude and direction of

Table 1
GPS site description and coseismic displacements

S. no.	Region	Site	Code	Long	Lat	Julian day of survey in 1995	Julian day of survey in 2004	Julian day of survey in 2005	Observed displacement (m)			Simulated displacement (m)		
									U_{East}	U_{North}	U_{Up}	U_{East}	U_{North}	U_{Up}
1	North Andaman	Aerial Bay	AB	93.027	13.278	–	58,75,94,96	15,17	−3.90 ± 0.04	−2.71 ± 0.01	0.49 ± 0.05	−3.46	−2.38	0.65
2		East Island	EI	93.047	13.631	–	75	17	−3.62 ± 0.04	−2.51 ± 0.02	0.96 ± 0.07	−3.69	−2.58	0.46
3	Middle Andaman	Long Island	LI	92.932	12.376	–	58,61	15,16	−1.96 ± 0.02	−1.10 ± 0.01	−0.48 ± 0.06	−1.72	−1.03	−0.79
4		Udaygarh	UG	92.773	12.216	–	61	15,16	−2.39 ± 0.02	−1.66 ± 0.01	−0.36 ± 0.05	−1.85	−1.21	−0.41
5		Govindgarh	GG	92.983	12.036	78	63	16,17,22	−1.36 ± 0.05	−0.95 ± 0.02	−0.18 ± 0.02	−1.75	−0.78	−0.75
6	South Andaman	Port Blair	PB	92.721	11.649	66	58,63,77,94,96	11–22	−3.07 ± 0.02	−1.03 ± 0.01	−0.96 ± 0.06	−2.31	−1.16	−0.55
7		Passage Island	PI	92.676	11.178	–	77	22	−2.91 ± 0.02	−1.19 ± 0.01	−0.71 ± 0.05	−2.86	−1.42	−0.89
8	Little Andaman	Hut Bay	HB	92.569	10.696	–	77,79	18,19,20,22	−3.27 ± 0.01	−2.65 ± 0.01	−0.26 ± 0.02	−3.42	−2.67	−0.79
9[a]	Car Nicobar	Car Nicobar	CN	92.804	9.225	–	2003/244, 245	53,54	−5.76 ± 0.01	−2.95 ± 0.01	−1.11 ± 0.01	−5.72	−2.97	−1.44
10	Nicobar Islands	Teresa Island	TI	93.124	8.302	–	79,83	19	−5.86 ± 0.02	−3.06 ± 0.01	−2.85 ± 0.04	−5.60	−2.96	−2.82
11		Kardip	KD	93.549	8.036	–	83	19,20,21	−3.97 ± 0.02	−1.72 ± 0.01	−1.35 ± 0.04	−4.51	−2.10	−1.67
12		Miroe Island	MI	93.541	7.514	–	88	20	−4.91 ± 0.02	−2.84 ± 0.01	−2.16 ± 0.05	−4.92	−2.77	−2.72
13	Great Nicobar	Campbell Bay	CB	93.934	7.004	–	88,94,96	20	−4.10 ± 0.02	−2.36 ± 0.01	−1.60 ± 0.03	−4.14	−2.32	−1.91

[a] GPS data from CN site are from [17]. It was first occupied on September 1 and 2, 2003 before the earthquake and on 53 and 54 Julian day of 2005 after the earthquake.

coseismic displacements at the adjacent sites, we divided the rupture on the curved subduction zone into 14 rectangular segments. In each segment the slip was assumed to be uniform. Thus, the slip in our model varied along the strike direction of the rupture only. Dip of the rupture was assumed to be 12° under Andaman Island, 10–11° under Nicobar Islands and 8–9° further south [3]. The updip edge of the rupture is assumed to coincide with the trench axis. The strike of the rupture was assumed to coincide with the local strike of subduction zone at that site. For each segment, we estimated depth of the downdip edge of the rupture (or rupture width) and slip on the rupture. The initial guess for the above estimates is derived from a 2-D analysis in which the length of the rupture is assumed to be infinite in each segment. In Fig. 2, we show the variation of difference between the computed and observed horizontal and vertical displacements at CB while varying the slip and rupture width. Similar analysis was done for other sites as well. For horizontal displacement, slip decreases with increasing the rupture width, but not significantly when rupture width exceeds the distance between the updip edge of the rupture and the site. Analysis related to vertical displacement suggests that slip is minimum when the rupture width is equal to the distance between the updip edge of the rupture and the site. The slip increases significantly by increasing or decreasing the rupture width. Contours of minima of analysis of the horizontal and vertical displacements (Fig. 2) generally provide two estimates of slip and rupture width (Table 2). These estimates were used as initial models in the analysis in which the rupture length in each segment is now considered finite. The slip and the downdip width of each rectangular rupture plane were again estimated in such a way so as to minimize the difference between the observed and predicted coseismic horizontal and vertical surface displacements at all sites using trail and error approach. Fig. 3 shows the observed and predicted displacements at some sites in Andaman–Nicobar region. Similar graphs can be shown for other sites as well. Besides the good fit between the observed and simulated displacements, it predicts uplift at the North Sentinel Island and on the west coast of the Andaman Islands [11,21,22]. The coseismic displacement vector directions are towards SWS, except at HB, where it is more towards SW. The slip vectors too are oriented towards SWS, except in Middle and South Andaman. This could be real as the tectonics in this region is more complex because of the presence of spreading system in the back-arc basin (Fig. 1), which is characterised by low shear wavespeed and low shear wavespeed and bulk-sound speed ratio [24].

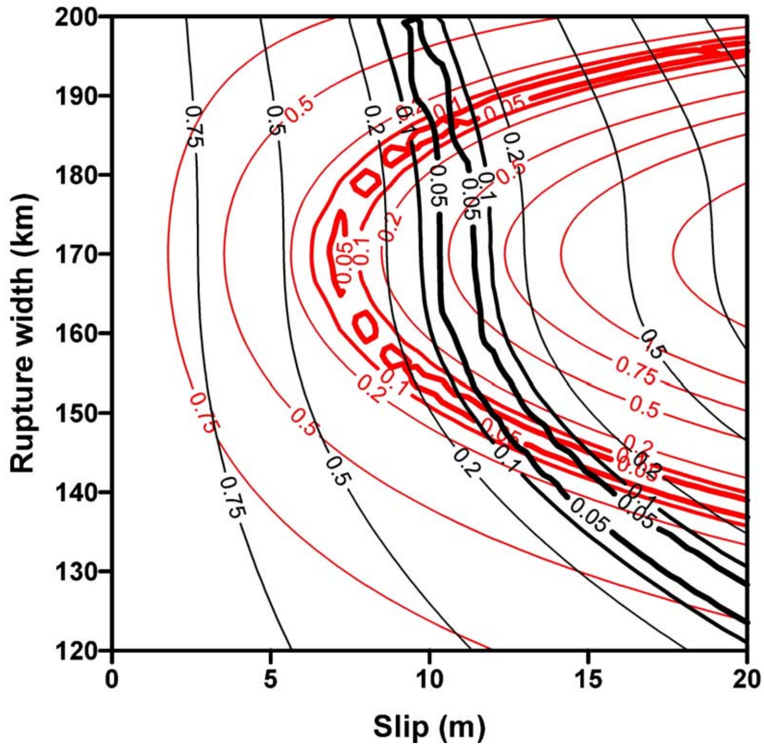

Fig. 2. Contours of difference between the observed and computed horizontal (black) and vertical (red) displacement, normalised by the observed horizontal and vertical displacement at CB, respectively. We carried out similar exercise at other sites also. Analysis of horizontal and vertical displacements at each site generally provides two estimates of slip and rupture width corresponding to the two common minima. (For interpretation of the references to colour in this figure legend, the reader is referred to the web version of this article.)

Large displacements in the Andaman–Nicobar Islands are not very sensitive to the slip on the southern part of the rupture, i.e., south of 6°N, hence the slip on this part is not well resolved. For this portion of the rupture we assumed a simple slip model, which is generally consistent with that derived from the seismological and far-field geodetic data. In this model, high slip of 16 m is assumed near 4°N [3,12]. In our esti-

Table 2
Estimates of slip and rupture width

S. no.	Site	Initial model derived from 2-D analysis				Final model	
		Slip (m)	Rupture width (km)	Slip (m)	Rupture width (km)	Slip (m)	Rupture width (km)
1	EI	–	–	6.5	<200	7.9	149
2	AB	–	–	7.2	158	7.9	149
3	GG	–	–	10.6	74	3.8	118
4	LI	4.8	132	8.9	86	3.8	118
5	UG	5.6	119	18.0	61	3.8	118
6	PB	7.3	119	10.0	86	5.6	122
7	PI	7.0	122	11.5	80	5.6	122
8	HB	7.6	122	–	–	7.7	122
9	CN	13.6	159	–	–	14.8	156
10	KD	10.7	194	12.7	146	15.1	148
11	TI	15.2	150	16.2	129	15.1	148
12	MI	12.6	162	14.8	133	15.1	156
13	CB	10.4	186	13.3	147	11.3	155

Initial model has been derived from 2-D analysis in which rupture length under each site was assumed to be infinite. This analysis generally provided two estimates of rupture width and slip. One of these estimates is close to the final model. Estimates derived from GG, UG and KD from 2-D analysis are not appropriate, as these sites lie east of LI and TI, respectively, in the same segment.

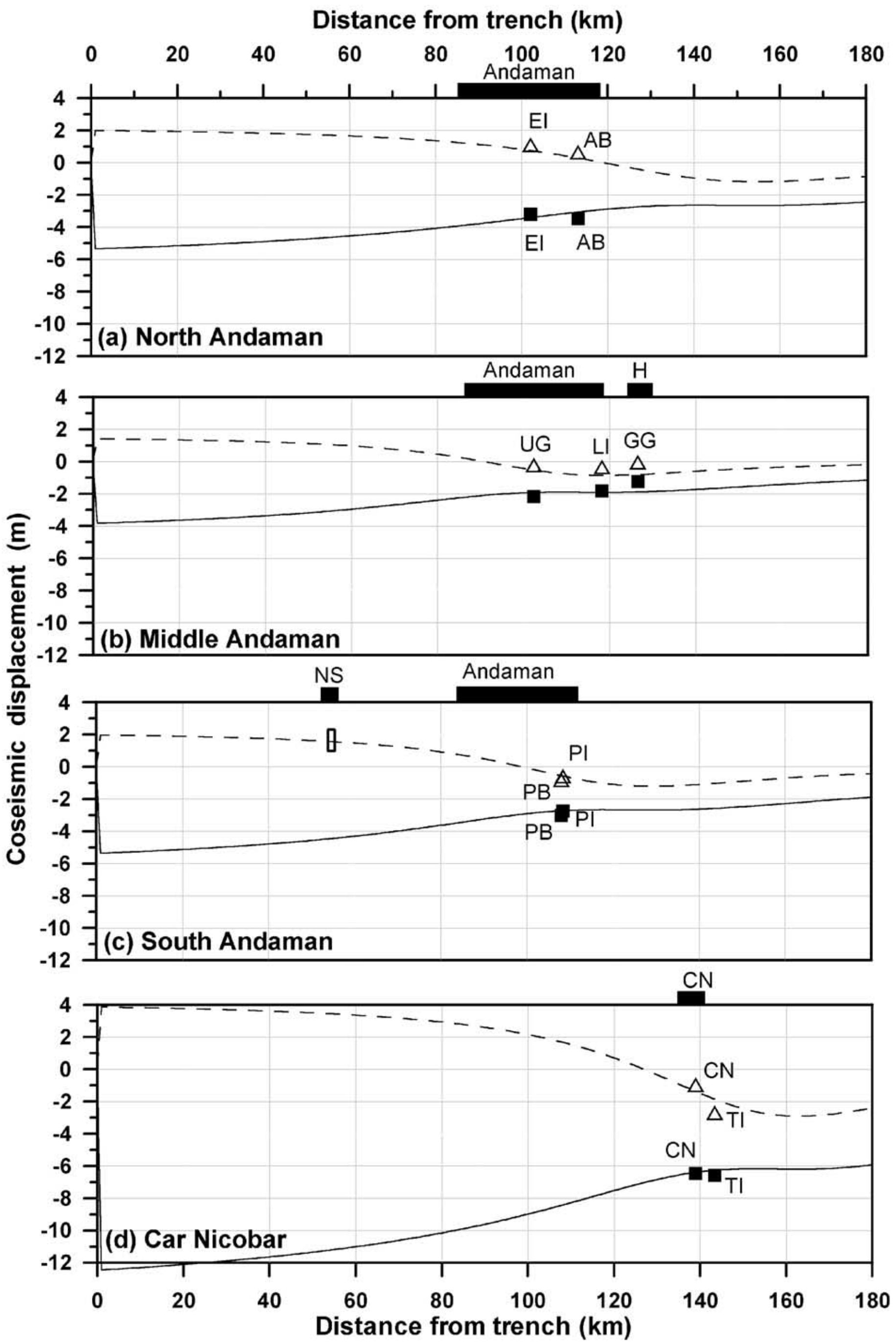

Fig. 3. Variation of coseismic displacement at GPS sites with distance from trench in Andaman and Nicobar islands. Simulated trench normal horizontal (continuous curves) and vertical (dashed curves) displacements correspond to the slip model of Fig. 1. The analysis predicts uplift at sites EI and AB, on the western coast of Andaman Islands, and on N. Sentinel Island (NS) [11,21,22]. H—Havelock Island, CN—Car Nicobar Island.

mated rupture model under the Andaman–Nicobar Islands, maximum slip of 15.1 ± 0.2 m (15 m thrust and 1.8 m dextral slip) on rupture occurred between Great Nicobar and Car-Nicobar Islands, i.e., between 7 and 9°N latitudes. Models derived from seismic waveform analysis [12,15,25] also predict relatively high slip in this region. The downdip width of rupture in this part varies between 135 and 156 km (Table 2). The slip decreased in the north direction and was 4–8 m under Little and South Andaman Island. Here the downdip width of the rupture varies between 122 and 149 km only (Table 2). Further north, under Middle Andaman Island, slip is estimated as 3.8 ± 0.2 m only (3.7 m thrust and 1.5 m dextral) on a 118 ± 5-km-wide rupture. The slip under the North Andaman is relatively high (7.9 ± 0.2 m with 6.5 m of thrust and 4.5 of dextral slip) as compared to adjacent Middle Andaman region. Uplift at the two northernmost stations EI and AB requires that the downdip edge of the rupture be shifted towards the east. Thus, in this part, either the width of rupture increased or the rupture shifted towards east. The second possibility seems to be more likely, as the subduction zone here slightly swings towards east. The slip in the Andaman Islands is very oblique to the subduction zone. Our analysis requires that the rupture extended at least up to 14°N but whether it extended further north, cannot be resolved from the data.

The scalar moment release in Andaman–Nicobar region for this earthquake in our model is 4.5×10^{22} Nm (M_w 9). The average root mean squared error between the observed and predicted displacement is 0.32 m. The model is consistent with the reported coseismic displacements in Thailand, Indonesia and Malaysia [3]. For example, at Phuket our model predicts a displacement of 29 cm, consistent with the reported displacement of 27 cm. We did not use GPS data from far-field IGS stations [14,16], as this will require consideration of a spherical earth model [14] whereas our analysis assumes earth to be homogeneous elastic half space.

In the analysis of seismological data to estimate the slip on rupture, a dip of 17.5° for the rupture under the Andaman has been assumed which decreases to 12° near its southern edge [2,12]. We also considered this estimate of dip and estimated the variation of slip and rupture width along the rupture in Andaman–Nicobar region. The consideration of increase in dip leads to increase in slip at all segments. This is due to the fact that all the sites lie close to the downdip edge of the rupture and higher dip of rupture places the downdip edge of the rupture at deeper depth level, which leads to higher estimation of coseismic slip. However, the increase in dip does not simulate the far-field displacements and predicts more displacement than observed. Hence, we preferred a gentle dip, varying from 8° in the south to 12° in the north.

High slip seems to coincide with the bend in the subduction zone. The two large patches of high slip, near 4° and 8°N coincide with 25–30° fault bends. The relatively high-slip region in the North Andaman also coincides with a bend. The rupture was apparently arrested at this point. Relatively lower slip and smaller rupture width under the South and Middle Andaman islands is intriguing and may possibly be related with the last major earthquake in the region that occurred in 1941 [13]. The surface projection of the downdip edge of the rupture appears to approximately coincide with the Eastern Margin Fault (EMF) in the Andaman Nicobar Islands and with the West Andaman Fault (WAF) in the region further south of it [4].

4. Postseismic deformation

Rapid postseismic transients for several major and great subduction zone earthquakes have been reported [26–28], which occur over a time scale of days to decades. As discussed earlier, GPS measurements at Port Blair during January 11 to 22, 2005 were made throughout the survey campaign. The 12-day data at Port Blair (PB in Fig. 1) show apparent transients (Fig. 4). These observations suggest that during this period Port Blair continued to move in the direction of coseismic displacement and in 12-day period it moved by 4.1 cm (i.e., at a rate of about 1.2 m/yr) toward N259°. Though the errors are large in the vertical component, it appears that uplift occurred in this period, whereas subsidence occurred during the coseismic period. During this period, no strong aftershock occurred in the Andaman region; hence, we assume that the entire motion is due to postseismic deformation caused by the mainshock. We estimate that this postseismic displacement corresponds to an afterslip of about 10–12 cm on the downdip part of the rupture. Similar transients following the earthquake have also been observed at sites in Thailand, Indonesia and Malaysia [3] and other campaign mode sites in Andaman and Nicobar Islands (Jade, 2005; C.D. Reddy, 2005, personal communication).

5. Interseismic deformation during 1995–2004

As discussed above, SOI initiated GPS measurements in Andaman–Nicobar region in 1994–1995 and hence measurements at Port Blair (PB) and Govindgarh (GG) during March 1995 are available. Data from other sites could not be retrieved. The 1995–2004 observations at PB and GG provide a velocity of about 44 ± 6 mm/yr towards N339° in ITRF2000 and a relative velocity of about 63 ± 6 mm/yr towards N277° with respect to Indian plate. Large errors in the estimate are due to the shorter duration (7 h) of GPS measurements during the 1995 campaign. Paul et al. [7] reported campaign mode GPS measurements at CARI, a different site in Port Blair, which were made during four campaigns in 1996, 1998 and 1999. The velocity of this site in ITRF2000 is estimated as 45.2 ± 3 towards N50° [29]. Though the

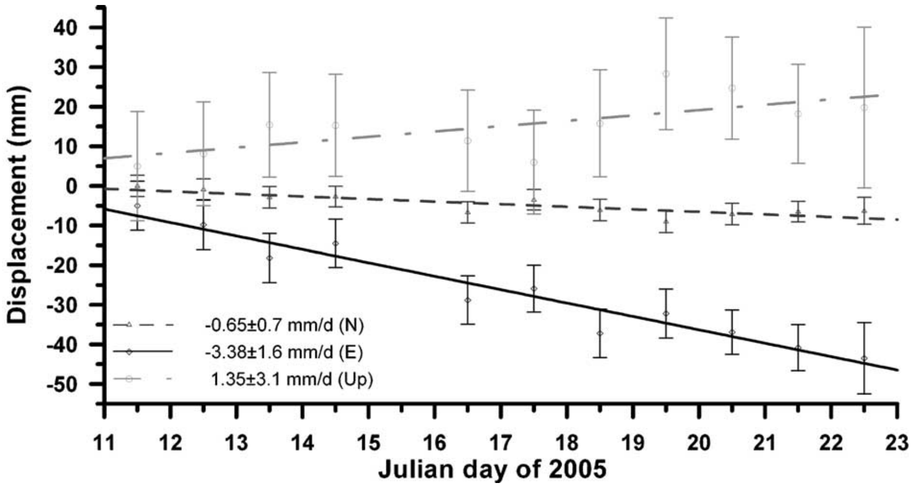

Fig. 4. North (N), East (E) and vertical (U) components of post-seismic transients at Port Blair (PB). Straight lines are the best-fit lines in least square sense. During the period of observation from January 11 to 22, the GPS site at Port Blair moved 41 mm towards N259°.

two estimates are consistent in magnitude, the direction of motion differs significantly, which indicates intense variation in strain accumulation both in time and space. Thus, none of these estimates represent the actual plate motion as both estimates are based on the measurements made during the period of strain accumulation. The velocity at CARI with respect to Indian plate is about 13.3 ± 3 mm/yr towards N250° [29]. Using an elastic half space model, we estimated that this velocity corresponds to a back-slip of about 23 ± 6 mm/yr on a fully locked subduction zone with the downdip width of about 120 km under the Andaman Island. The 1995–2004 data set provides extremely high rate of strain accumulation on the same part of the locked zone, which is about four–five times of the above estimate, suggesting that the rate of strain accumulation varied with time. However, possibility exists that portion of locked region on subduction zone changed with time. Limited observations from only two sites do not allow us to further explore these possibilities. In any case, high strain accumulation rates varying from 16 to 68 mm/yr have been reported from the west Sumatra subduction zone [8–10]. Thus, it appears that the rate of strain accumulation in the Andamans was fast and probably varied significantly both in space and time in past 10 yr.

6. Seismic hazard implications

6.1. Earthquake triggering near the southern edge of the rupture

Tectonics and earthquake occurrence processes at the southern and northern edges of the rupture appear complex. The earthquake nucleated close to the southern edge of the rupture and propagated in the north direction only. Aftershocks were abundant in the region north of the southern edge of the rupture, but almost no aftershocks occurred immediately southeast of the southern edge, i.e., in the source region of the March 28, 2005 great earthquake. It has been argued that the 2004 earthquake and subsequent viscoelastic relaxation increased stresses in the region southeast of the rupture [30–32], which triggered the March 28, 2005 earthquake. The process of stress transfer by the giant 2004 earthquake to the abutting region of 2005 earthquake without causing any aftershocks in the source region of 2005 earthquake, in the period between the two earthquakes, is intriguing. The region between the two abutting ruptures approximately coincides with the Wharton Fossil ridge of age about 40 Ma, flanked by the oceanic floor of age up to 100 Ma on either side of the ridge, high thermal anomaly [33], and with the diffused India–Australia plate boundary. This region possibly acted as some kind of heterogeneity between the two ruptures.

6.2. Earthquake triggering near the northern edge of the rupture

The rupture in the north terminated just north of North Andaman Island. Whether the earthquake can trigger a great or major earthquake adjacent to its northern edge, in the subduction zone between the North Andaman and Indo-Burmese Arc region (i.e., between 14° and 21°N latitude), in a manner similar to the southern edge of the rupture, where it triggered the 2005 earthquake [30–32] may be debated. We suggest that the processes of earthquake occurrence and plate motion are more complex further north of the rupture. The age of the subducting plate increases from about 60 to 90 million yr between Sumatra in the south and Andaman in the north, which may alter the mechanical coupling between the two plates [2]. The presence of this barrier probably did not allow the rupture to propagate further north. The transition from oceanic to continental lithosphere, south of Indo-Burmese arc [34], may also affect the subduction process. Further, a change in strike of the subduction zone along the Andamans, which becomes almost parallel to the plate motion in the Andaman region and north of it, leads to predominantly strike-slip motion as compared to predominantly thrust motion in the south. GPS measurements in the Myanmar region reveal that the arc-parallel motion between the Indian and Sunda plates is shared between the Sagaing fault in the east and Indo-Burmese arc in the west with insignificant thrust motion across the plate boundary [35]. It has also been suggested that the pole of rotation between India and Burmese plates lies at [36] or slightly east [1] of the northern edge of the rupture. Thus, the convergence direction becomes strike-slip at the northern rupture edge, which probably explains why the rupture ceased at that end [1]. Kennett and Cummins [24] ascribed to the presence of physical barrier. They suggested that the change in morphology of the subduction zone, which is associated with the changes in physical properties, modified the distribution of slip along the rupture. Further they identified three prominent physical barriers along the arc, which are characterized by the low ratio of shear wavespeed and bulk sound speed. The first barrier, near Great Nicobar, coincides with the region, which approximately marked the northern edge of the rupture associated with fast slip [2]. The second barrier lies just south of the Andaman Islands, where significant change in the strike of subduction zone occurs. The third barrier lies immediately north of the Andaman Islands, which probably caused termination of rupture at northern end.

Though major earthquakes have occurred in the Indo-Burmese arc region, no great or even major earthquakes have occurred in the intervening subduction zone between North Andaman and Indo-Burmese Arc region, i.e., between 14° and 21°N latitudes. All the above factors probably suggest that the 2004 earthquake may not trigger a great or major earthquake in the northern extension of the subduction zone.

Acknowledgement

Discussions with Roland Bürgmann, Chris Vigny, Seth Stein, Jean-Phillipe Avouac, Mohamed Chlieh, Kerry Sieh, Aron Meltzner, Kalpna, C. Subramaniam and R.K. Chadha helped in greatly improving the manuscript. Suggestions from an anonymous reviewer are gratefully acknowledged. We thank Rob D. van der Hilst, the editor of EPSL, for his prompt and supportive handling of the manuscript. We thank Surveyor General of Survey of India and Director, NGRI for permission to publish the work. The work was financially supported by Department of Science and Technology.

References

[1] S. Stein, E.A. Okal, E.A. Speed, Speed and size of the Sumatra earthquake, Nature 434 (2005) 581–582.
[2] T. Lay, et al., The Great Sumatra–Andaman Earthquake of 26 December 2004, Science 308 (2005) 1127–1133.
[3] C. Vigny, et al., Insight into the 2004 Sumatra–Andaman earthquake from GPS measurements in southeast Asia, Nature 436 (2005) 201–206.
[4] J.R. Curray, Tectonics and history of the Andaman sea region, J. Asian Earth Sci. 25 (2005) 187–228.
[5] R. McCaffrey, Oblique plate convergence, slip vectors, and forearc deformation, J. Geophys. Res. 97 (B6) (1992) 8905–8915.
[6] K. Sieh, D. Natawidjaja, Neotectonics of the Sumatran fault, Indonesia, J. Geophys. Res. 105 (2000) 28,295–28,326.
[7] J. Paul, et al., The motion and active deformation of India, Geophys. Res. Lett. 28 (2001) 647–650.
[8] L. Prawirodirdjo, Y. Bock, R. McCaffrey, J. Genrich, E. Calais, C. Stevens, S.S.O. Puntodewo, C. Subarya, J. Rais, P. Zwick, Geodetic observations of interseismic strain segmentation at the Sumatra subduction zone, Geophys. Res. Lett. 24 (21) (1997) 2601–2604, doi:10.1029/97GL52691.
[9] M. Simoes, J.P. Avouac, R. Cattin, P. Henry, The Sumatra subduction zone: a case for a locked fault zone extending into the mantle, J. Geophys. Res. 109 (B10402) (2004) doi:10.1029/2003JB002958.
[10] Y. Bock, L. Prawirodirdjo, J.F. Genrich, C. Stevens, R. McCaffrey, C. Subarya, S.S.O. Puntodewo, E. Calais, Crustal motion in Indonesia from GPS measurements, J. Geophys. Res. 108 (2003) 2367, doi:10.1029/2001JB000324.
[11] R. Bilham, E.R. Engdahl, N. Feldl, S.P. Satyabala, Partial and complete rupture of the Indo-Andaman plate boundary 1847–2004, Seismol. Res. Lett. 76 (2005) 299–311.
[12] C.J. Ammon, et al., Rupture process of the 2004 Sumatra–Andaman earthquake, Science 308 (2005) 1133–1139.
[13] R. Bilham, A flying start, then a slow slip, Science 308 (2005) 1126–1127.
[14] P. Banerjee, F.F. Pollitz, R. Bürgmann, The size and duration of the Sumatra–Andaman earthquakes from far-field static offsets, Science 308 (2005) 1769–1772.
[15] M. Ishii, P.M. Shearer, H. Houston, J.E. Vidale, Extent, duration and speed of the 2004 Sumatra–Andaman earthquake imaged by Hi-Net array, Nature 435 (2005), 933–936.
[16] J.K. Catherine, V.K. Gahalaut, V.K. Sahu, Constraints on rupture of the December 26, 2004, Sumatra earthquake from far-field GPS observations, Earth Planet. Sci. Lett. 237 (2005) 673–679.
[17] S. Jade, M.B. Ananda, S. P. Dileep Kumar, S. Banerjee, Coseismic and postseismic displacements in Andaman and Nicobar Islands from GPS measurements, Cur. Sci. 88 (2005) 1980–1984.

[18] R. King, Y. Bock, Documentation for the GAMIT GPS Analysis Software, Release 9.94, Mass. Inst. of Technol., Cambridge, Mass. and Scripps Inst. of Oceanogr., La Jolla, Calif., 2000.

[19] T. Herring, Global Kalman Filter VLBI and GPS Analysis Program (GLOBK), version 5.0, Mass. Inst. of Technol., Cambridge, Mass, 2000.

[20] B. Nagarajan, S. Kumar, J.K. Catherine, V.K. Gahalaut, Coseismic displacements in Andaman–Nicobar Island due to 26 December 2004 Sumatra earthquake, Journal of Earth System Science (in press).

[21] V.K. Gahalaut, R.K. Chadha, Sumatra tsunamogenic earthquake of 26 December 2004, Deep Cont. Stud. Depart. Sci. Technol. Newsl. 15 (1) (2005) 18–20.

[22] A.J. Meltzner, K. Sieh, M. Abrams, D.C. Agnew, K.W. Hudnut, J.P. Avouac, D.H. Natawidjaja, Uplift and subsidence associated with the Great Aceh-Andaman earthquake of 2004, J. Geophys. Res. (in press).

[23] Y. Okada, Internal deformation due to shear and tensile faults in a half space, Bull. Seismol. Soc. Amer. 82 (1992) 1018–1040.

[24] B.L.N. Kennett, P.R. Cummins, The relationship of the seismic source and subduction zone structure for the 2004 December 26 Sumatra–Andaman earthquake, Earth and Planetary Science Letters (in press).

[25] I.V. Fine, A.B. Robinovich, R.E. Thomson, The dual source region for the 2004 Sumatra tsunami, Geophys. Res. Lett. 32 (2005) L16602, doi:10.1029/2005GL023521.

[26] T.I. Melbourne, F.H. Webb, J.M. Stock, C. Reigber, Rapid postseismic transients in subduction zones from continuous GPS, J. Geophys. Res. 107 (B10) (2002) 2241, doi:10.1029/2001JB000555.

[27] R. Bürgmann, M.G. Kogan, V.E. Levin, C.H. Scholz, R.W. King, G.M. Steblov, Rapid aseismic moment release following the 5 December, 1997 Kronotsky, Kamchatka, earthquake, Geophys. Res. Lett. 28 (2001) 1331–1334.

[28] S. Miyazaki, K.M. Larson, K. Choi, K. Hikima, K. Koketsu, P. Bodin, J. Haase, G. Emore, A. Yamagiwa, Modeling the rupture process of the 2003 September 25 Tokachi-Oki (Hokkaido) earthquake using 1-Hz GPS data, Geophys. Res. Lett. 31 (2004) L21603, doi:10.1029/2004GL021457.

[29] S. Jade, Estimates of plate velocity and crustal deformation in the Indian subcontinent using GPS geodesy, Current Science, 86, 1443–1448.

[30] J. McCloskey, S.S. Nalbant, S. Steacy, Earthquake risk from coseismic stress, Nature 434 (2005) 291.

[31] S.S. Nalbant, S. Steacy, K. Sieh, D. Natwidjaja, J. McCloskey, Earthquake risk on the Sunda trench, Nature 435 (2005) 756–757.

[32] V.K. Gahalaut, Kalpna, 28 March 2005 Sumatra earthquake: triggered, expected, aftershock?, Curr. Sci. 89 (2005) 452–454.

[33] M.H. Ritzwoller, N.M. Shapiro, E.R. Engdahl, Structural context of the Great Sumatra–Andaman Islands earthquake, submitted for publication.

[34] U. Chandra, Tectonic segmentation of the Burmese–Indonesian arc, Tectonophysics 105 (1984) 279–290.

[35] A. Socquet, C. Vigny, N. Chamot-Rooke, C. Rangin, W. Simons, B. Ambrosius, Indian Plate's motion and deformation induced along its boundary with Sunda in Myanmar determined by GPS J Geophys. Res. 2005JB003877 (in press).

[36] P. Bird, An updated digital model of plate boundaries, Geochem. Geophys. Geosyst. 4 (2003) 1027, doi:10.1029/2001GC000252.